THE EFFECT OF BOULDER CONTACT ON MOMENTUM TRANSFER EFFICIENCY IN THE DART IMPACT G. S. Collins[1], K. Dai[1], T. M. Davison[1], S. D. Raducan[2], A. M. Stickle[3]. [1]Department of Earth Science and Engineering, Imperial College London, SW7 2BP, UK, g.collins@imperial.ac.uk. [2]University of Bern, Switzerland; [3]Johns Hopkins Applied Physics Laboratory, Laurel, MD.

Introduction: The successful deflection of asteroid Dimorphos by the DART spacecraft impact [1] provides an important test of numerical impact codes. It also offers an opportunity to better understand the role of asteroid internal structure and surface properties on impact cratering and momentum transfer [2]. The poignant final images returned to Earth by the DART spacecraft, moments before impact, revealed that the surface of Dimorphos is dominated by large boulders, comparable to or bigger than the DART spacecraft, including two very close to the projected impact location [1]. With some notable exceptions [e.g., 2, 3], most pre-mission modelling studies represented the target as a continuum [2]. Laboratory experiments have shown that large boulders can have an "armoring" effect, dissipating some impact energy and reducing crater size [e.g., 4-8]. However, the effect on momentum transfer of large boulders, particularly those in direct contact with the spacecraft, is not well understood. Here we investigate the effect of a single boulder at the impact point on momentum transfer for an idealised DART impact scenario.

Numerical Modelling: We simulate a DART-like impact using the iSALE shock physics code [9-11]. A complete assessment of the effect of surface boulders on the impact requires a fully 3D simulation in which multiple interacting boulders are represented. While such efforts are ongoing by the DART Impact Modelling Group, here we employ a highly simplified approach to investigate the influence of a single boulder at or below the impact point on a vertical impact on an otherwise homogeneous target. This scenario can be efficiently simulated with a 2D axially symmetric cylindrical geometry (Fig. 1). Our simulation set-up is based on previous iSALE2D simulations of the DART impact [12-14]. The spacecraft bus is represented as a thin-shelled hollow cylinder of height and diameter 0.8 m and mass 630 kg, impacting vertically at $U = 6.5$ km/s. The target is represented as a weak, porous regolith-like material into which a single boulder is embedded at or below the impact point. A Tillotson equation of state for basalt is used to represent the solid regolith and boulder materials. Strength and porosity model parameters for the regolith were kept fixed; a porosity of 20% and a weak cohesive strength of 10 Pa was assumed for the regolith. A nominal porosity 7.4% and intact cohesive strength of 1 MPa was assumed for the boulder; however, the qualitiative effect of the boulder on ejecta production was not sensitive to these properties, so long as the boulder was assumed to be significantly stronger and less porous than the regolith. The effect on ejecta production of boulder size, position (top of boulder relative to surface), strength and porosity were investigated.

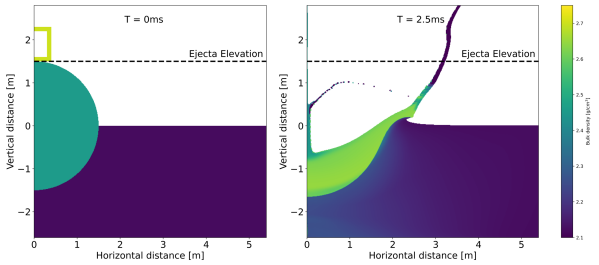

Figure 1: Head-on collision of DART spacecraft bus with a half-buried, 3-m diameter boulder in a weak, porous regolith. Impactor momentum is transferred to the regolith via the boulder, modulating the transfer efficiency.

Ejecta properties (mass, launch velocity and momentum) were recorded using tracer particles as they crossed a specified elevation (the top of the boulder; Fig. 1). The very weak strength (10 Pa) of the regolith resulted in prolonged crater growth and ejection and hence very long simulation times, even when regridding was used. However, as the relative effect of the boulder on ejecta production is clearly evident before the end of crater growth, here we compare ejecta distributions and momentum transfer efficiencies at a fixed time of two seconds after impact when the crater has reached approximately half its final diameter.

Results: Our simulations show that boulder position and size can substantially affect the ejecta mass-velocity distribution and momentum transfer efficiency of the impact (Figs. 2, 3). For the nominal case of a 3-m diameter boulder, two important differences in ejecta production are evident when the boulder protrudes above the surface, compare with the no boulder case (Fig. 2). First, direct contact between the boulder, which is denser and stronger than the regolith, produces a greater mass of high-speed ejecta than is produced when there is no boulder at the impact point (Fig. 2). While this high speed ejecta does not make a substantial contribution to the total ejecta momentum, it will dictate the expansion speed of the front of the ejecta plume. The second, more important, effect is that disruption of the boulder dissipates some of the impact energy before it couples with the regolith target resulting in a smaller mass of low-speed ejecta from the regolith compared with the no boulder scenario (Fig. 2). This armoring effect, which

has been previously observed in laboratory experiments [4-8], is particularly important for momentum transfer as most of the ejected momentum belongs to the low-speed ejecta. After two seconds of crater growth, the effect of armoring can reduce the total ejected momentum by as much as a half (Fig. 3).

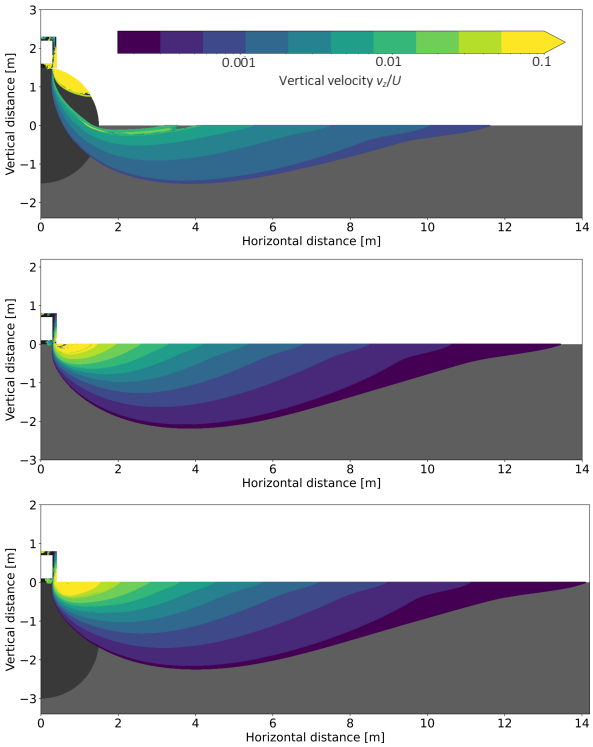

Figure 2: Comparison of provenance of ejecta as a function of vertical ejection velocity for a half-buried boulder (top); no boulder (middle) and a fully submerged boulder (bottom).

Our simulations also considered the case of a fully buried or submerged boulder. In this case, the effect of the boulder on ejecta production is very different. The presence of the boulder, with greater stiffness, greater strength and higher impedance than its surroundings, in the coupling zone where the impactor transfers its energy and momentum to the target, actually leads to an amplification of cratering efficiency and ejection speeds. This results in more high-speed ejecta, originating from the boulder and proximal near surface, as well as more low-speed ejecta (Fig. 2c). This is because the boulder dissipates less impact energy than the equivalent volume of regolith does when the boulder is absent. This "anti-armoring" regime of ejection velocity amplification occurs when the boulder is almost entirely buried, or is entirely buried but where its top is within one boulder radius of the surface (Fig. 3). The maximum amplification of ejected momentum observed in our simulations after two seconds of crater growth was about 25% for a boulder buried just below the surface.

The armoring and anti-armoring effects of the impacted boulder are sensitive to the size of the boulder (Fig. 3). For boulders less than half the diameter of the spacecraft, the anti-armouring effect was not observed and the armoring effect was substantially reduced. The armoring effect is significant for boulders with a diameter more than 10-20% of the spacecraft diameter.

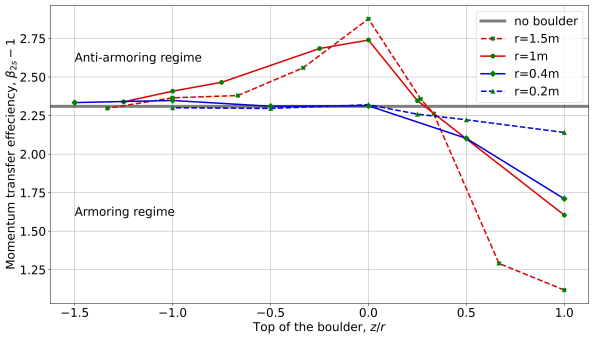

Figure 3: Relative total momentum of ejecta launched in first two seconds compared to the no-boulder case (grey line) as a function of boulder size and normalized position (elevation of top of boulder relative to surface divided by boulder radius *r*).

Conclusion: Numerical simulations of a head-on collision of the DART spacecraft with a single boulder embedded in an asteroid surface reveal that the size and vertical position of the boulder can have a significant effect on the speed, mass and momentum of ejecta and therefore the total momentum transfer (deflection) efficiency. An impacted boulder with more than 25% of its diameter above the surface provides an armoring effect, reducing momentum transfer efficiency, while a boulder buried just below the surface can amplify the momentum of the ejecta and hence momentum transfer.

Acknowledgments: We gratefully acknowledge the developers of iSALE (www.isale-code.de). This work was supported by STFC (ST/S000615/1).

References: [1] Daly RT, et al., (2022) *Nature*, submitted. [2] Stickle AM, et al. (2022) *PSJ*, 3: 248. [3] Raducan SD, et al. (2022) Ast. & Atrophys, 665: L10. [4] Güttler C, et al. (2012) *Icarus* 220: 1040–1049. [5] Tatsumi E and Sugita S. (2018). *Icarus* 300: 227–248. [6] Barnouin OS, et al. (2019) *Icarus* 325: 67–83. [7] Yasui M, et al. (2022) *JGR-Planets,* 127: e2021JE007172. [8] Okawa H, et al. (2022) *Icarus*, 387: 115212. [9] Amsden AA et al. (1980) SALE: Simplified ALE LANL Report LA-8905. Los Alamos, New Mexico, 101 p. [10] Collins GS et al. (2004) *Meteoritics & Planet. Science.* 9(2): 217–31. [11] Wünnemann K et al. (2006) *Icarus* 180(2): 514–27. [12] Raducan SD, et al. (2019) *Icarus* 329: 282-295. [13] Raducan SD, et al. (2020) *Planet Space Sci.* 180, 104756. [14] Raducan SD, et al. (2022) Int. J. Impact. Eng. 162: 104147.